Malaysian Journal of Chemistry, 2026, Vol. 28(1), 20-30
(Special Issue: *3rd International Conference on Industry-Academia Initiatives in Biotechnology & Chemistry, iCIABC2025*)

Effects of Temperature, Duration, and Solution Conditions on Physicochemical Properties, Antioxidant Activity, and Volatile Carbonyl Compounds in Glucosamine Caramels

Ai Chee, Chan[1,2], Siti Umairah, Mokhtar[1] and Pui Khoon, Hong[1,3]*
[1]Faculty of Industrial Sciences and Technology, Universiti Malaysia Pahang Al-Sultan Abdullah, Lebuhraya Persiaran Tun Khalil Yaakob, 26300 Gambang, Kuantan, Pahang, Malaysia
[2]Politeknik Sultan Haji Ahmad Shah, Semambu, 25250 Kuantan, Pahang, Malaysia
[3]Centre for Bioaromatic Research, Universiti Malaysia Pahang Al-Sultan Abdullah, Lebuhraya Persiaran Tun Khalil Yaakob, 26300 Gambang, Kuantan, Pahang, Malaysia
*Corresponding author (e-mail: hongp@umpsa.edu.my)

The non-enzymatic browning of glucosamine (GlcN) generates advanced glycation end-products (AGEs) and volatile carbonyl compounds (VCCs), which have both beneficial and detrimental health effects. This is the first systematic study investigating how high temperature and solution type affect the caramelisation of GlcN, which participates in both Maillard and caramelisation reactions. Caramels were produced by incubating GlcN (20% w/v) in water, phosphate, or acetate buffers at 80, 100, and 120 °C for one or two hours. Physicochemical properties, antioxidant activity, and VCCs profiles were evaluated. Browning progression, indicated by absorbance at 280, 320, and 420 nm, revealed concurrent formation of pre-melanoidins and melanoidins. Acetate-buffered caramels exhibited the darkest colour, highest pH, and significantly greater antioxidant activity (ABTS and DPPH, $p<0.05$). In contrast, water-based systems produced the highest levels of 5-hydroxymethylfurfural (5-HMF) at 120 °C for 2 h. Methylglyoxal and glyoxal were the most abundant in acetate-based samples at 100 °C for 1 h, while diacetyl concentrations were comparable across systems at 120 °C. The presence of reactive carbonyls and AGE precursors highlights both functional potential and safety considerations in GlcN-derived caramels. Overall, GlcN caramelisation offers a promising natural antioxidant but warrants attention to thermal and compositional control for safe application.

Keywords: Antioxidant activity, buffer effects, glucosamine caramel, non-enzymatic browning, volatile carbonyl compounds

Received: June 2025; Accepted: November 2025

Non-enzymatic browning (NEB) encompasses complex chemical reactions, primarily the Maillard reaction and caramelisation. The Maillard reaction occurs between reducing sugars and amino groups of biomolecules such as peptides and nucleic acids under mild conditions. Caramelisation requires higher temperatures for sugar degradation. Both reactions can occur simultaneously during thermal food processing. It contributes to the development of characteristic pigments (melanoidins), as well as volatile and non-volatile compounds that influence flavour and aroma quality [1].

In the Maillard reaction, reducing sugar reacts reversibly with amino compounds to create a Schiff bases, which rearrange into Amadori products. These intermediates undergo two main pathways: under acidic conditions (pathway I), forming 3-deoxyhexasone and 5-hydroxy-2-methylfurfural (5-HMF); under alkaline conditions (pathway II), producing glyoxal (GO), methylglyoxal (MGO), diacetyl (DA), and related intermediates [2]. DA, GO, and MGO are also found in the blood of diabetic patients. Further interaction of sugar and amino groups leads to high molecular weight products like melanoidin, which contribute to the colour of caramel [3]. Caramelisation typically begins with the dehydration of sugars, followed by isomerisation and fragmentation reactions [4]. These processes generate a variety of volatile and non-volatile compounds, such as furans, aldehydes, acids, and polymers, which contribute to the characteristic brown colour and complex flavour of caramelised products [5, 6].

Although NEB plays a crucial role in the biochemical transformations observed during thermal processing of food and biological tissues. However, if not properly controlled, NEB can create undesirable secondary metabolites, including AGEs. AGEs can be developed endogenously in the hum an body and exogenously in processed and stored food. Their accumulation has been linked to oxidative stress, cytotoxicity and chronic disease pathogenesis in biological systems [2-4].

†Paper presented at the 3rd International Conference on Industry-Academia Initiatives in Biotechnology & Chemistry

GlcN, an amino sugar with both aldehyde and amino groups, can undergo Maillard-like self-condensation reactions and caramelisation even at moderate temperatures (25-37 °C) [10, 11]. This reactivity makes it an interesting model compound for studying complex browning phenomena and a potential source of functional ingredients. Studies have shown that heating GlcN solutions leads to significant colour development, pH reduction, resembling caramel formation [12]. GlcN-derived caramels also exhibit antioxidant activity, primarily due to melanoidins and bioactive compounds like fructosazine and deoxyfructosazine, which possess potential anti-diabetic and anti-inflammatory properties [11, 12]. Notably, studies under sous-vide processing have shown that GlcN caramelisation can yield low or undetectable levels of typical precursors of AGEs like 4-methylimidazole, 2-acetyl-4-tetrahydroxybutylimidazole, and 5-HMF [11].

However, most research has focused on mild conditions, leaving the effects of higher temperature and buffer composition largely unexplored. This study addresses this gap by systematically investigating how temperature and buffer type influence GlcN caramelisation. The balance between the formation of beneficial antioxidant compounds and potentially detrimental VCCs is a key consideration for evaluating the potential of these caramels as functional food ingredients.

EXPERIMENTAL

Chemicals and Materials

All chemicals and standards were of analytical grade. D-GlcN hydrochloride, sodium acetate, glacial acetic acid (99.7%), sodium phosphate monobasic monohydrate (98.0%), and sodium phosphate dibasic heptahydrate (99.0%) were purchased from Alfa Aesar (USA).

Reagents for the antioxidant assays were sourced as follows: 2,2'-azino-bis (3-ethylbenzothiazoline-6-sulfonic acid) diammonium salt (ABTS, 98%) and 2,2-diphenyl-1-picrylhydrazyl (DPPH) were from Alfa Aesar (USA). (±)-6-Hydroxy-2,5,7,8-tetramethylchromane-2-carboxylic acid (Trolox, 97%) was from Sigma-Aldrich (Switzerland). Potassium persulfate (ACS reagent, 99.0%) and analytical grade ethanol (95%) were purchased from Merck (Darmstadt, Germany).

For the analysis of volatile carbonyl compounds (VCCs), O-(2,3,4,5,6-pentafluorobenzyl)-hydroxylamine (PFBHA) (≥98%) and a PDMS/DVB SPME fibre (65 µm) were acquired from Sigma-Aldrich (Switzerland). VCC standards, including DA (97%), GO (40% solution), MGO (40% solution), and 5-HMF (99%), were obtained from Sigma-Aldrich (China).

Preparation of GlcN Caramel

GlcN solutions were prepared in at high concentrations (20% w/v) by dissolving D-GlcN hydrochloride in one of three solutions: deionised water (W), 0.1 M phosphate buffer (P) (pH 6.8), or 0.1 M acetate buffer (A) (pH 5.6). The pH of all types of glucosamine solution was not adjusted before, during and after incubation. Aliquots (10 mL) of each GlcN solution were placed in sealed glass vials and incubated in a temperature-controlled oven at 80, 100, or 120 °C for either 1 or 2 hours. After the specified incubation period, the vials were immediately removed and cooled to room temperature. Samples were then further analysed. A total of 18 treatments were prepared. Each experimental condition was performed in triplicate.

Physicochemical Characterization

The pH of the GlcN solutions before incubation (initial pH) and the resulting caramel solutions after incubation (final pH) were measured at room temperature (25 ± 1 °C) using a digital pH meter (Mettler Toledo Seven Easy, Greifensee, Switzerland) equipped with a glass electrode. Before measuring the samples, the pH meter was calibrated with buffer pH 4 and 7.

UV-visible absorption spectra of the diluted 100-fold caramel solutions were recorded from 200-450 nm using a Shimadzu UV-1800 spectrophotometer. Deionised water was used as a blank [12]. Absorbance at 280, 320, and 420 nm was used to monitor early (GlcN condensation), intermediate (pre-melanoidins), and late-stage (melanoidins) browning products [15].

Colour was characterised using a colourimeter (Precise Colour Reader, HP-200, China) to determine CIELAB coordinates (L^* for lightness, a^* for redness-greenness, b^* for yellowness-blueness) and Chroma (C), representing colour saturation [16]. For testing, glucosamine caramels were pipetted into glass test tubes. The instrument was calibrated using a white ceramic plate for the white reading, followed by a black trap reading. The colour of the samples was measured with the colourimeter by determining the CIE L^*, a^*, b^* and C colour values.

Determination of Antioxidant Activity

The ABTS radical scavenging activity was determined following a modified method [17]. Briefly, the ABTS•+ solution was prepared by reacting a 7 mM ABTS solution with 2.45 mM potassium persulfate (1:1, v/v) and incubating the mixture in the dark at room temperature for 12-16 h. The resulting solution was diluted with 0.02 M sodium acetate buffer (pH 4.5) to achieve a final absorbance of 0.70 ± 0.01 at 734 nm. For the analysis, 20 µL of standard or sample was mixed with 3 mL of the ABTS working solution.

Caramel samples were analysed undiluted. After 30 min of incubation, the absorbance was recorded at 734 nm using a Thermo Scientific Genesys 10S UV-vis spectrophotometer. Measurements were corrected against a sample blank (20 µL sample in 3 mL acetate buffer).

The DPPH radical scavenging activity was assessed using a modified method [18]. A 0.1 mM DPPH solution in 95% ethanol was prepared. For the assay, 20 µL of standard or the undiluted caramel samples were added to 3 mL of the DPPH solution. The decrease in absorbance was measured at 517 nm after 30 minutes of incubation in the dark. All measurements were corrected using a sample blank (20 µL sample in 3 mL of 95% ethanol).

Both results were expressed as mM Trolox equivalents (TE) per mL of caramel (mM TE/mL), using a Trolox standard curve. The Trolox concentration range was 0.5 to 5 mM for ABTS and 1 to 7 mM for DPPH. The Trolox standard curve for the ABTS radical scavenging assay yielded the linear equation $y = -0.1647x + 0.702$ ($R^2 = 0.9988$), while the DPPH assay yielded $y = -0.1456x + 1.2328$ ($R^2 = 0.9966$), where y represents absorbance and x represents the Trolox concentration in mM.

Analysis of VCCs

VCCs, including DA, GO, MGO, and 5-HMF, were analysed using Headspace Solid-Phase Microextraction (HS-SPME) coupled with Gas Chromatography-Mass Spectrometry (GC-MS) following derivatisation with PFBHA [6,19]. A 1.9 mL standard / undiluted sample was incubated with 0.1 mL of 20 g/L PFBHA in a 20 mL headspace vial at room temperature for 7 min. After a 4-minute fibre pre-cleaning, volatiles were extracted using a 65 µm DVB/CAR/PDMS SPME fibre at 85 °C for 20 min and desorbed in the GC injector for 3 min.

GC-MS was performed using an Agilent 7890 GC with a 5975C MSD and an HP-5MS column (30 m × 0.25 mm, 0.25 µm). The injector was set to 250 °C (splitless); helium was used as the carrier gas (1.0 mL/min). The oven was programmed to 50 °C (1 min), then ramped to 200 °C at 5 °C/min, then to 250 °C at 20 °C/min. EI was used at 70 eV; the ion source and quadrupole were set at 150 °C and 230 °C, respectively. Spectra were recorded in full scan mode. The concentrations of DA, GO, and MGO were quantified in parts per billion (ppb), while the concentration of 5-HMF was quantified in parts per million (ppm) using external standard calibration curves. The linear regression equations and coefficients of determination (R^2) were DA, $y = 30{,}732{,}007{,}743x - 343{,}722{,}790$ ($R^2 = 0.9989$); GO, $y = 24{,}324{,}868{,}359x + 3{,}349{,}571$ ($R^2 = 0.9794$); MGO, $y = 56{,}948{,}397{,}723x + 7{,}607{,}012$ ($R^2 = 0.996$); and 5-HMF, $y = 51{,}362{,}046x - 767{,}546{,}409$ ($R^2 = 0.9751$). In all equations, y represents the peak area, and x represents the concentration.

Statistical Analysis

Data were expressed as means ± standard deviation from at least three replicates. Before analysis, data were screened for outliers using box plots, and the assumptions for ANOVA were verified. Normality of residuals was confirmed visually using Q-Q plots, and homogeneity of variances was assessed by plotting residuals versus predicted values. One-way ANOVA and Tukey's HSD post-hoc test were used to identify significant differences ($p<0.05$). Pearson's correlation and factorial ANOVA were performed using IBM SPSS Statistics (v22). The General Linear Model assessed the effects and interactions of temperature, solution, and time in GlcN caramel production. Contribution percentages were derived from the sum of squares. Tukey's test was used to identify whether specific significant group differences were appropriate.

RESULTS AND DISCUSSION

Reaction Conditions on Physicochemical Properties

For clarity in data presentation, samples were labelled based on solutions (W = water, P = phosphate, A = acetate), temperature (80, 100, 120 °C), and reaction time (1 h or 2 h). For example, W80_2h refers to a sample incubated in water at 80 °C for 2 hours.

pH Characteristic

The initial pH values of the GlcN solutions were 3.22 ± 0.01 for water, 4.77 ± 0.03 for sodium phosphate buffer, and 4.52 ± 0.03 for sodium acetate buffer. After incubation, a significant decline in pH was observed at 120 °C for all caramels (Figure 1), indicative of the formation of acidic by-products such as formic acid and acetic acid [10]. The decrease was most substantial in water-based caramels (e.g., W120_2h, pH 1.36 ± 0.05) ($p<0.05$). Notably, the pH of A120 was similar to P120 for both 1 and 2-hour durations at 120 °C. Acetate-based caramels generally maintained a higher pH at 80 °C and 100 °C, suggesting a stronger buffering capacity under those conditions compared to the phosphate and water systems [20]

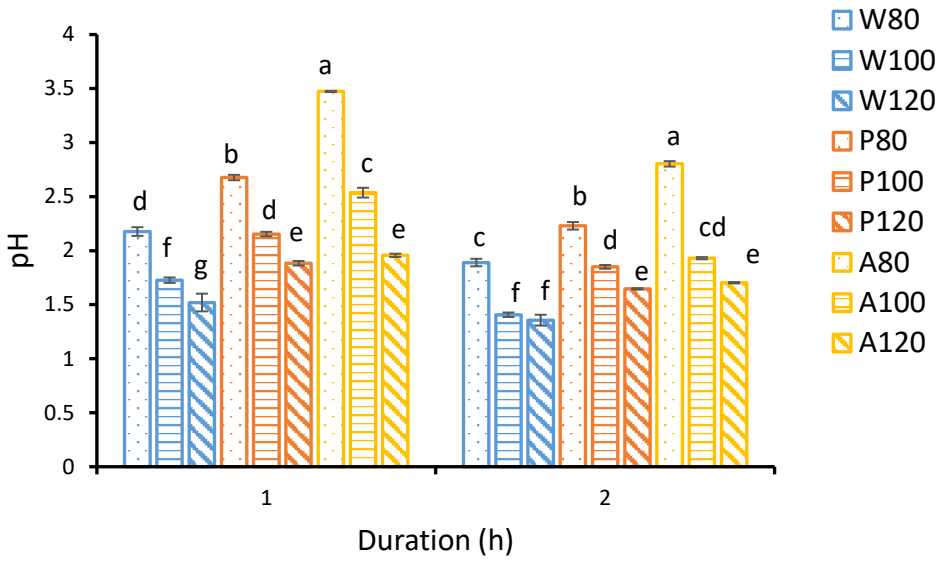

Figure 1. pH changes of GlcN caramel in water (W), sodium phosphate (P) and sodium acetate (A) at 80, 100 and 120 °C over 1 and 2 h.
Different superscript letters (a-f) within the same duration indicate significant differences ($p<0.05$).

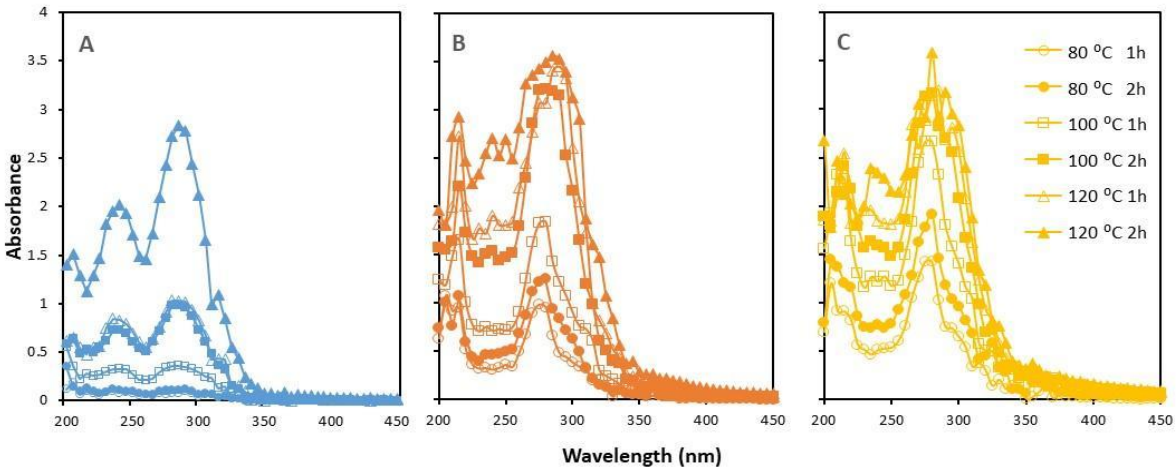

Figure 2. UV-vis absorption spectra of GlcN caramel prepared in water (A), sodium phosphate (B) and sodium acetate (C).

UV-visible Spectroscopy

Browning progression (Figure 2) showed characteristic absorbance for early (280 nm), intermediate (320 nm), and late-stage (420 nm) products. The absorption intensity of water-based caramels was generally low compared to other caramels. P120_2h showed the highest absorption intensity at 280 and 320 nm, while acetate-based caramels (A100, A120) dominated at 420 nm, indicating more advanced melanoidin formation ($p<0.05$). The concurrent formation of products detected at wavelengths highlights the rapid and overlapping stages of browning in the highly reactive GlcN system [21].

CIELAB Colour Space

As shown in Table 1 and Figure 3, increasing temperature and time led to darker caramels (lower L^* values). Acetate-based caramels (e.g., A120_2h, L^*=25.13±0.13) and phosphate-based caramels at 120 °C (e.g., P120_2h, L^*=25.52±0.05) were the darkest.

Table 1. Changes in colour characteristics *L** and *C* in caramel samples.

Caramel	Time, h	*L**	*C*
W80	1	51.72 ± 1.84[a]	17.90 ± 1.26[c]
	2	50.49 ± 1.33[a]	18.10 ± 0.47[c]
W100	1	49.63 ± 0.89[a]	20.50 ± 0.87[b]
	2	46.00 ± 0.28[b]	24.17 ± 0.60[a]
W120	1	44.21 ± 0.71[b]	23.40 ± 0.61[a]
	2	30.76 ± 0.57[c]	9.65 ± 0.21[d]
P80	1	41.53 ± 0.60[a]	24.52 ± 0.67[a]
	2	38.36 ± 0.57[b]	19.67 ± 0.89[b]
P100	1	32.33 ± 0.27[c]	11.57 ± 0.86[c]
	2	28.26 ± 0.41[d]	5.30 ± 0.27[d]
P120	1	26.38 ± 0.17[e]	3.16 ± 0.33[e]
	2	25.52 ± 0.05[e]	0.67 ± 0.09[f]
A80	1	34.86 ± 0.45[a]	14.88 ± 0.33[a]
	2	27.50 ± 0.13[b]	4.39 ± 0.16[b]
A100	1	26.22 ± 0.23[c]	2.56 ± 0.14[c]
	2	25.48 ± 0.20[d]	0.49 ± 0.11[f]
A120	1	25.30 ± 0.26[d]	0.84 ± 0.03[de]
	2	25.13 ± 0.13[d]	1.32 ± 0.19[d]

W: water, P: sodium phosphate solution and A: sodium acetate solution
Different superscript letters (a-f) within the same solution type indicate significant differences ($p < 0.05$) among samples.

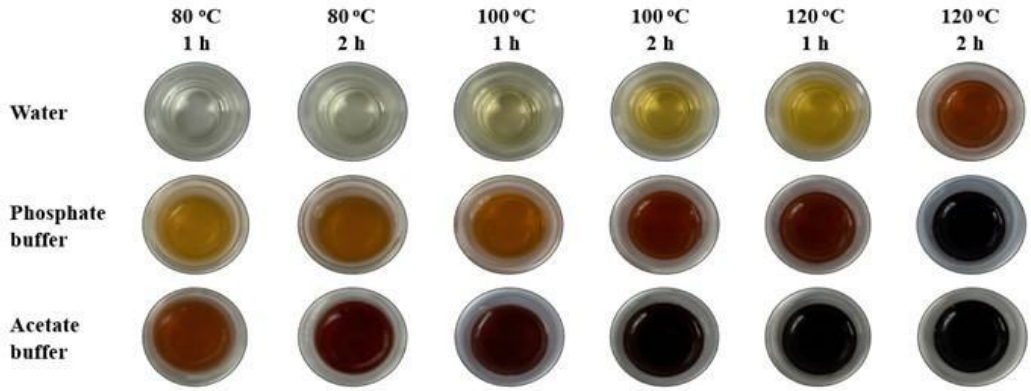

Figure 3. Colour development of 20% GlcN caramel in water, sodium phosphate and sodium acetate at 80, 100 and 120 °C after 1 and 2 hours of heating.

The chromaticity plot (Figure 4) illustrates the shift in colour tones (a^* vs. b^*). Water-based caramels remained in the greenish-yellow quadrant ($a^* < 0$, $b^* > 5$), except for W120_2h, which shifted towards reddish-yellow tone. In contrast, buffered systems, particularly at high temperatures, transitioned from reddish-yellow ($a^* > 0$, $b^* > 0$) to reddish-blue or greenish-blue ($b^* < 0$), indicating significant pigment structure changes.

Chroma (colour purity, *C*) in water-based caramels increased up to 100 °C but dropped significantly at 120 °C (Table 1). In buffered systems, *C* generally decreased with increasing temperature and time as colours became darker and less saturated. The pronounced browning in acetate-based caramels suggests a catalytic effect of the acetate ion on pigment formation [20].

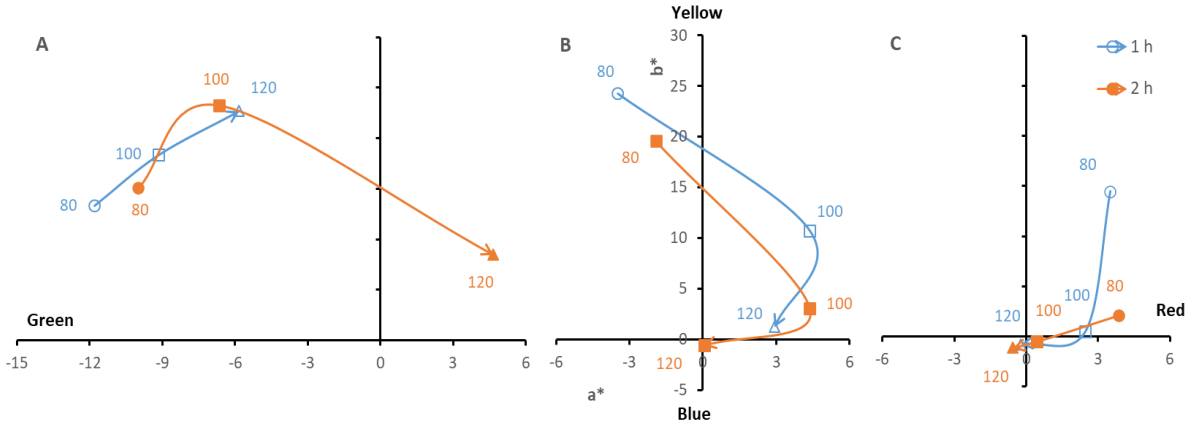

Figure 4. *a** vs. *b** chromaticity plot showing the effect of treatment time (1 and 2 h) at 80, 100, and 120 °C on GlcN caramel prepared with water (A), sodium phosphate (B), and sodium acetate (C).

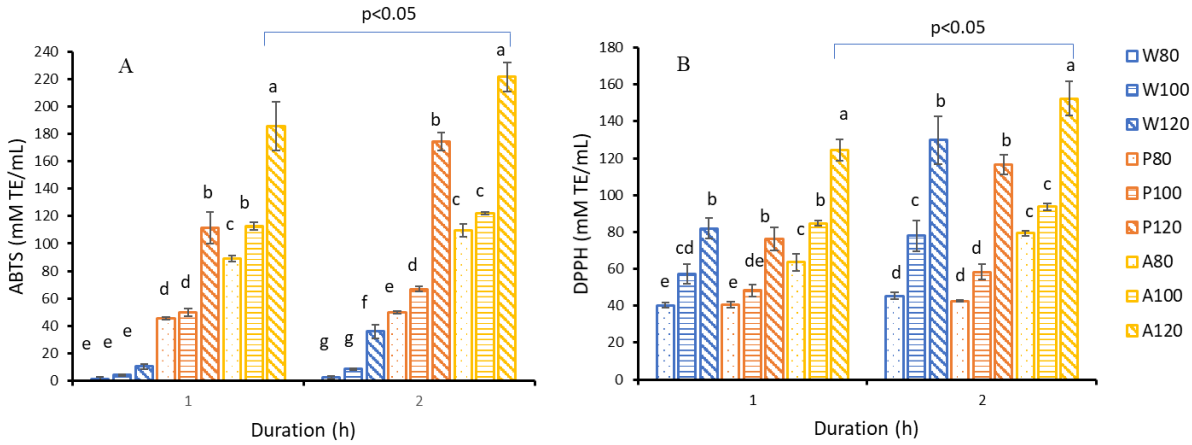

Figure 5. Antioxidant capacity of GlcN caramels prepared in water (W), sodium phosphate (P), and sodium acetate (A) at 80, 100, and 120 °C for 1 and 2 h, as measured by (A) ABTS and (B) DPPH radical scavenging assays (expressed as mM Trolox equivalents/mL).
Different letters (a-g) within the same time duration (1 h or 2 h) indicate significant differences ($p < 0.05$) among samples.

Antioxidant Activity of GlcN Caramels

Acetate-based caramels consistently demonstrated the highest antioxidant activity in both ABTS and DPPH assays (Figure 5). Antioxidant activity increased with temperature and time, peaking in the A120_2h samples (ABTS: 221.62±10.59 mM TE/mL; DPPH: 152.42±9.14 mM TE/mL). This was significantly higher ($p < 0.05$) than that of phosphate- or water-based caramels under identical conditions.

The superior antioxidant activity in acetate-based systems points to specific catalytic effects of acetate or the reaction environment, potentially due to the role of the acetate ion in promoting enolization and fragmentation pathways [20]. This environment favours the efficient formation of high molecular weight products, such as potent radical scavenging melanoidins [15], which were confirmed by the highest 420 nm absorbance observed in acetate-based caramels.

Profile of VCCs

The VCCs analysed as potential AGE precursors were DA, GO, MGO, and 5-HMF. Table 2 presents the derivatised volatiles in caramels, along with retention times and m/z ions. E/Z isomers were observed due to the PFBHA derivatisation, resulting in slightly different retention times [19]. Identification was confirmed using standards and mass spectra.

Table 2. Compounds, retention time and identified ions of volatile compounds in caramel.

Derivatised Compound	Retention time (min)	Ions (m/z)
DA	25.77 / 27.18 / 28.99	279 and 476
GO	27.46 / 27.63	251 and 448
MGO	27.07 / 27.78 / 28.10 / 28.32	265 and 462
5-HMF	26.49 / 26.71	123 and 321

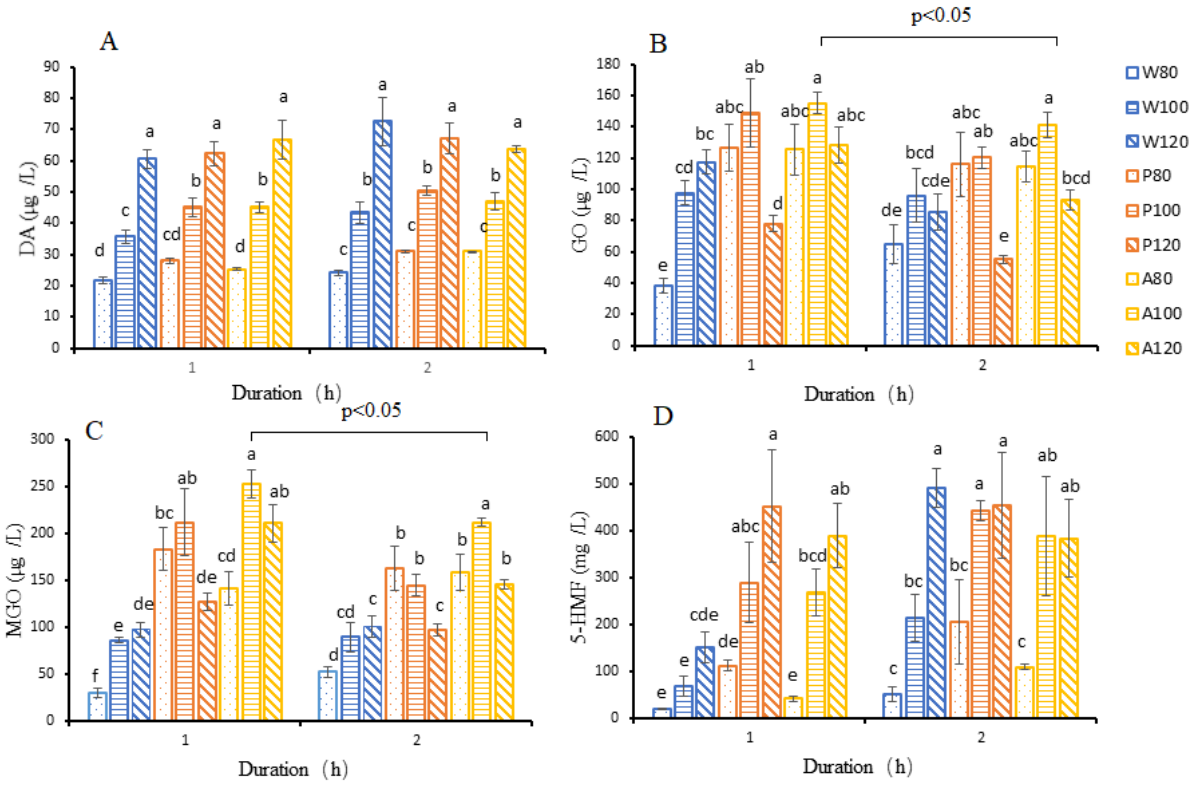

Figure 6. Levels of VCCs: (A) DA (µg/L), (B) GO (µg/L), (C) MGO (µg/L), and (D) 5-HMF (mg/L) in GlcN caramels prepared in water (W), sodium phosphate (P), and sodium acetate (A) at 80, 100, and 120 °C for 1 and 2 h.
Different letters (a-f) within the same time duration (1 h or 2 h) indicate significant differences ($p < 0.05$) among samples.

DA concentrations ranged from 21.63 to 72.59 µg/L across the samples, indicating moderate variability among treatments (Figure 6A). Levels of DA were similar for all caramel types prepared at 120 °C for both 1 and 2-hour durations. Caramels produced at 80 and 100 °C also showed similar DA levels in the second hour across the three buffer types. DA content increased with temperature: 120 °C > 100 °C > 80 °C ($p<0.05$). Temperature was the dominant factor, with DA content increasing significantly with temperature ($p < 0.05$). Buffer type had less effect, with most systems showing comparable DA levels at 120 °C. Compared to previous studies using HPLC methods, higher DA levels were reported up to 12.4 mg/L in iron-catalysed systems [14], 32 mg/L with GlcN-glycine [22], and 2.2 mg/L at lower temperatures [13]. Compared to previous studies, these DA levels were lower.

GO levels (38.26 to 155.25 µg/L) showed complex trends (Figure 6B). Generally, GO levels were higher in the 1st-hour caramels compared to the 2nd-hour. A sharp decrease in GO was noted in phosphate-based caramels at 120 °C. The highest GO levels were seen in acetate- and phosphate-buffered samples at 100 °C. Previous studies reported GO levels in GlcN caramels varying widely—from 0.3 to 34.9 mg/L—with some studies detecting no GO under

UV-C treatment [10, 11, 13, 22]. These levels fall within the wide range reported previously.

MGO was present in even broader concentrations, ranging between 29.66 and 252.67 µg/L (Figure 6C). The highest concentrations of MGO were found in acetate-buffered samples at 100 °C for both 1-hour and 2-hour durations. The lowest levels were consistently in the W80 samples. For water-based, MGO increased from 80 to 100 °C, then remained consistent from 100 to 120 °C (both durations). In buffered systems, MGO increased from 80 to 100 °C, then decreased at 120 °C for both durations. Previous studies reported a wide range of MGO levels in GlcN models, from non-detectable to 57.7 mg/L [10, 11, 13, 21], whereas this study showed markedly lower levels.

Among the VCCs, 5-HMF showed the greatest variation, ranging widely from 19.1 to 490.61 mg/L (Figure 6D). In the water-based system, 5-HMF formation was strongly temperature-dependent, increasing significantly at 120 °C. At 2h, W120 (490.61±41.99 mg/L) > W100 (213.02±50.28 mg/L) > W80 (50.29±15.63 mg/L) ($p<0.05$). The highest level was found in W120_2h. This study observed significantly higher 5-HMF levels than previous reports [21], likely due to elevated temperatures (80–120 °C) and acidic conditions (pH < 4) that enhance sugar degradation, promoting 5-HMF formation [2,6,24].

These findings present a critical trade-off: acetate-buffered conditions produced the highest antioxidant activity but also generated significant levels of AGE precursors like MGO (Figure 6B and 6C). This contrasts with water-based systems, which produced the most 5-HMF but had lower MGO and GO. This highlights a key challenge for food safety: conditions that maximise functional properties (antioxidants) may not align with those that minimise the formation of potentially detrimental compounds.

Correlation Analysis

Table 3 presents Pearson's correlations between physicochemical, antioxidant, and VCCs properties in GlcN caramels. This revealed a strong correlation among browning intensity, colour, antioxidant activity, and VCCs in GlcN caramels. Absorbance at 280 nm showed strong inverse correlations with L^* (r = –0.926), b^* (r = –0.814), and chroma (r = –0.854), and a positive correlation with a^* (r = 0.750), indicating darker, redder colours with increased browning. Similar trends were observed at 320 nm and 420 nm. These wavelengths also correlated positively with DPPH (r = 0.684–0.836) and ABTS (r = 0.789–0.936), confirming that higher browning intensity was associated with greater antioxidant potential [25].

Among VCCs, DA and 5-HMF showed strong positive correlations with browning (e.g., at 280 nm, r = 0.757 and 0.854, respectively and at 320 nm, r = 0.784 and 0.723) and DPPH activity (r = 0.800 and 0.619). Higher DA and 5-HMF showed higher antioxidant [25, 26]. GO strongly correlated with MGO (r = 0.872), reflecting linked formation pathways. Buffer type and temperature influence caramel properties. Caramels treated at 120 °C in acetate buffer had the darkest colour and strongest antioxidant activity—emphasising the impact of low pH and heat in NEB outcomes [28].

Table 3. Pearson's correlation analysis on the physicochemical properties (pH, browning intensity and colour), antioxidant properties (ABTS and DPPH), and volatile carbonyl compounds (DA, GO, MGO and 5-HMF) in the glucosamine caramels.

Pearson Correlation	pH	280nm	320nm	420nm	L^*	a^*	b^*	C	ABTS	DPPH	DA	GO	MGO	5-HMF
pH	1	-.164	-.270*	-.211	-.085	.262	.029	.015	.091	-.396**	-.616**	.365**	.374**	-.462**
280nm	-.164	1	.840**	.777**	-.926**	.750**	-.814**	-.858**	.789**	.684**	.757**	.221	.482**	.854**
320nm	-.270*	.840**	1	.893**	-.777**	.500**	-.739**	-.769**	.852**	.836**	.784**	-.109	.192	.723**
420nm	-.211	.777**	.893**	1	-.731**	.341*	-.774**	-.789**	.936**	.779**	.646**	-.035	.313*	.630**
L^*	-.085	-.926**	-.777**	-.731**	1	-.860**	.845**	.896**	-.838**	-.622**	-.598**	-.364**	-.646**	-.730**
a^*	.262	.750**	.500**	.341*	-.860**	1	-.577**	-.645**	.522**	.353**	.423**	.491**	.630**	.587**
b^*	.029	-.814**	-.739**	-.774**	.845**	-.577**	1	.992**	-.803**	-.603**	-.503**	-.050	-.384**	-.634**
C	.015	-.858**	-.769**	-.789**	.896**	-.645**	.992**	1	-.832**	-.625**	-.538**	-.115	-.447**	-.671**
ABTS	.091	.789**	.852**	.936**	-.838**	.522**	-.803**	-.832**	1	.711**	.508**	.147	.484**	.538**
DPPH	-.396**	.684**	.836**	.779**	-.622**	.353**	-.603**	-.625**	.711**	1	.800**	-.044	.147	.619**
DA	-.616**	.757**	.784**	.646**	-.598**	.423**	-.503**	-.538**	.508**	.800**	1	-.001	.150	.823**
GO	.365**	.221	-.109	-.035	-.364**	.491**	-.050	-.115	.147	-.044	-.001	1	.872**	.075
MGO	.374**	.482**	.192	.313*	-.646**	.630**	-.384**	-.447**	.484**	.147	.150	.872**	1	.323*
5-HMF	-.462**	.854**	.723**	.630**	-.730**	.587**	-.634**	-.671**	.538**	.619**	.823**	.075	.323*	1

*. Correlation is significant at the 0.05 level (2-tailed).

**. Correlation is significant at the 0.01 level (2-tailed).

L^*: Lightness, a^*: Red-green value, b^*: Yellow-blue value, C: Chroma (colour intensity)

DA: diacetyl, GO: glyoxal, MGO: methylglyoxal and 5-HMF: 5-hydroxymethyl-2-furfural

Table 4. Contribution of various factors (%) and their interactions on the physicochemical properties (pH, browning intensity and colour), antioxidant properties (ABTS and DPPH), and volatile carbonyl compounds (diacetyl, glyoxal, methylglyoxal and 5-hydroxymethyl-2-furfural) in the glucosamine caramels.

Factors	pH	280 nm	320 nm	420 nm	*L**	*a**	*b**	*C*	ABTS	DPPH	DA	GO	MGO	5-HMF
Temperature (T)	47.5***	43.5***	60.6***	42.4***	22.8***	8.0***	19.4***	21.7***	24.1***	61.5***	91.7***	20.5***	10.6***	53.2***
Solution (S)	31.5***	40.2***	21.4***	34.0***	64.0***	48.9***	41.4***	47.0***	64.7***	21.7***	1.3**	28.8***	60.5***	15.3***
Time (t)	12.1***	5.3***	7.1***	3.8***	4.1***	1.5***	4.6***	5.0***	2.3***	9.1***	1.8***	4.7***	2.7***	9.8***
T × S	6.3***	2.8***	5.0***	16.4***	4.5***	28.3***	23.4***	17.4***	6.3***	0.7*	1.3**	29.8***	14.6***	2.6
T × t	1.0***	2.3***	2.9***	1.9***	0.20***	0.8***	1.1***	0.9***	1.3***	4.2***	0.02	3.9**	2.4**	0.9
S × t	1.0***	1.8***	0.3*	0.9***	0.7***	6.1***	0.3***	0.1**	0.3***	0.2	0.5*	1.7*	3.1***	2.0*
T × S × t	0.3***	3.6***	1.8***	0.3***	3.5***	5.2***	9.5***	7.7***	0.4**	0.7*	0.8*	1.8	1.5*	5.8**
ERROR	0.3	0.5	1.0	0.3	0.3	1.3	0.2	0.3	0.6	1.9	2.6	8.8	4.7	10.4
TOTAL	100.0	100.0	100.0	100.0	100.0	100.0	100.0	100.0	100.0	100.0	100	100	100	100

Contribution = Sum of squares from each factor / total corrected sum of squares
*L**: Lightness, *a**: Red-green value, *b**: Yellow-blue value, *C*: Chroma (colour intensity), hue: hue angle (colour tone) DA: diacetyl, GO: glyoxal, MGO: methylglyoxal and 5-HMF: 5-hydroxymethyl-2-furfural
* $p<0.05$
** $p<0.01$
*** $p<0.001$

Factorial ANOVA and Caramel Selection

Table 4 presents the factorial ANOVA results, showing the effects of temperature (T), solution (S), time (t), and their interactions on GlcN caramel properties. Temperature was the dominant factor, significantly influencing pH (47.5%), browning (absorbance at 280 nm: 43.5%; 320 nm: 60.6%; 420 nm: 42.4%), DPPH activity (61.5%), DA (91.7%), and 5-HMF (53.2%). The solution type mainly affected colour parameters (*L**: 64.0%; *a**: 48.9%; *b**: 41.4%; *C*: 47.0%), MGO (60.5%), and ABTS activity (64.7%). Although interaction effects were generally lower, T × S notably influenced GO (29.8%).

CONCLUSION

This study is among the first systematic evaluations of high-temperature (80–120 °C) GlcN caramelisation under different buffer conditions. The key finding is that buffer type significantly directs the reaction pathways. Specifically, acetate-based caramel produced at high temperature (120 °C) significantly enhances antioxidant activity and colour development, suggesting a preferential pathway for antioxidant compound formation. However, this optimal condition for functional properties presents a critical trade-off, as acetate buffer model also promotes the formation of AGE precursors like MGO. In contrast, non-buffered (water) systems produced the highest levels of 5-HMF at 120 °C but had lower antioxidant capacity. These findings underscore the complex balance between developing desirable functional attributes and ensuring food safety. Future research should focus on identifying the specific antioxidant compounds, assessing sensory attributes, and evaluating the safety implications of the VCC levels in acetate-buffered caramels for potential food applications.

ACKNOWLEDGEMENTS

This research was supported by financial funding from Universiti Malaysia Pahang Al-Sultan Abdullah under the PGRS230357 grant. The authors would also like to express their sincere appreciation to Institut Pengajian Siswazah, Universiti Malaysia Pahang Al-Sultan Abdullah (UMPSA) for sponsoring the conference participation fee for the 3rd International Conference on Industry-Academia Initiatives in Biotechnology and Chemistry 2025 (ICIABC 2025).

REFERENCES

1. Gupta, S., Sood, M., Gupta, N., Bandral, J. D. and Langeh, A. (2022) Food Browning, Its Type and Controlling Measures: A Review Article. *Chemical Science Review and Letters*, **11(44)**, 417–424.

2. Zhou, Z. and Langrish, T. (2021) A review of Maillard reactions in spray dryers. *Journal of Food Engineering*, **305**, 110615. https://doi.org/10.1016/j.jfoodeng.2021.110615.

3. BeMiller, J. N. (2019) Nonenzymic browning and formation of acrylamide and caramel. *Carbohydrate Chemistry for Food Scientists*, 351–370. https://doi.org/10.1016/B978-0-12-812069-9.00018-2.

4. Şen, D. and Gökmen, V. (2022) Kinetic modeling of Maillard and caramelization reactions in sucrose-rich and low moisture foods applied for roasted nuts and seeds. *Food Chem.*, **395**, 1–13. https://doi.org/10.1016/J.FOODCHEM.2022.133583.

5. Aydın, N., Kian-Pour, N. and Toker, O. S. (2021) Caramelized white chocolate: effects of production process on quality parameters. *Journal of Food Measurement and Characterization*, **15**, 3182–3194. https://doi.org/10.1007/s11694-021-00890-1.

6. Chan, A. C., Mokhtar, S. U. and Hong, P. K. (2025) A systematic review on the determination and analytical methods for furanic compounds in caramel models. *J. Food Sci. Technol.* https://doi.org/10.1007/s13197-025-06419-4.

7. Gerrard, J. (2005) The Maillard Reaction: Chemistry, Biochemistry and Implications by Harry Nursten. *Aust. J. Chem.*, **58**. https://doi.org/10.1071/ch0505_br.

8. Ozgolet, M., Yaman, M., Zeki Durak, M. and Karasu, S. (2022) The effect of five different sourdough on the formation of glyoxal and methylglyoxal in bread and influence of in vitro digestion. *Food Chem.*, **371**. https://doi.org/10.1016/j.foodchem.2021.131141.

9. Pal, R. and Bhadada, S. K. (2023) AGEs accumulation with vascular complications, glycemic control and metabolic syndrome: A narrative review. *Bone*, **176**. https://doi.org/10.1016/j.bone.2023.116884.

10. Ogutu, B., Kim, Y. -J., Kim, D. -W., Oh, S. -C., Hong, D. -L. and Lee, Y. -B. (2017) Optimization of Maillard reaction between glucosamine and other precursors by measuring browning with a spectrophotometer. *Prev. Nutr. Food Sci.*, **22**, 211–215. https://doi.org/10.3746/pnf.2017.22.3.211.

11. Zou, F., Hrynets, Y., Roopesh, M. S. and Betti, M. (2022) "Cold caramelization" of glucosamine under UV-C radiation. *Food Chemistry Advances*, **1**, 100083. https://doi.org/10.1016/j.focha.2022.100083.

12. Hong, P. K. and Betti, M. (2016) Non-enzymatic browning reaction of glucosamine at mild conditions: Relationship between colour formation, radical scavenging activity and α-dicarbonyl compounds production. *Food Chem.,* **212**, 234–243. https://doi.org/10.1016/j.foodchem.2016.05.170.

13. Hrynets, Y., Bhattacherjee, A., Ndagijimana, M., Hincapie Martinez, D. J. and Betti, M. (2016) Iron (Fe^{2+})-catalyzed glucosamine browning at 50 °C: Identification and quantification of major flavor compounds for antibacterial activity. *J. Agric. Food Chem.*, **64**, 3266–3275. https://doi.org/10.1021/ACS.JAFC.6B00761/SUPPL_FILE/JF6B00761_SI_001.PDF.

14. Dhungel, P., Hrynets, Y. and Betti, M. (2018) Sous-vide nonenzymatic browning of glucosamine at different temperatures. *J. Agric. Food Chem.*, **66**, 4521–4530. https://doi.org/10.1021/acs.jafc.8b01265.

15. Wu, S., Dai, X., Shilong, F., Zhu, M., Shen, X., Zhang, K., et al. (2018) Antimicrobial and antioxidant capacity of glucosamine-zinc(II) complex via non-enzymatic browning reaction. *Food Sci. Biotechnol.*, **27**, 1–7. https://doi.org/10.1007/s10068-017-0192-1.

16. Echavarría, A., Pagán, J. and Ibarz, A. (2016) Kinetics of color development in glucose/Amino Acid model systems at different temperatures. *Scientia Agropecuaria*, **7**, 15–21. https://doi.org/10.17268/sci.agropecu.2016.01.02.

17. Ilyasov, I. R., Beloborodov, V. L., Selivanova, I. A. and Terekhov, R. P. (2020) ABTS/PP decolorization assay of antioxidant capacity reaction pathways. *Int. J. Mol. Sci.*, **21**. https://doi.org/10.3390/ijms21031131.

18. Ozgen, M., Reese, R. N., Tulio, A. Z., Scheerens, J. C. and Miller, A. R. (2006) Modified 2,2-azino-bis-3-ethylbenzothiazoline-6-sulfonic acid (ABTS) method to measure antioxidant capacity of selected small fruits and comparison to ferric reducing antioxidant power (FRAP) and 2,2'-diphenyl-1- picrylhydrazyl (DPPH) methods. *J. Agric. Food Chem.*, **54**, 1151–1157. https://doi.org/10.1021/jf051960d.

19. Moreira, N., Araújo, A. M., Rogerson, F., Vasconcelos, I., Freitas, V. De. and Pinho, P. G. de. (2019) Development and optimization of a HS-SPME-GC-MS methodology to quantify volatile carbonyl compounds in Port wines. *Food Chem.*, **270**, 518–526. https://doi.org/10.1016/j.foodchem.2018.07.093.

20. Rizzi, G. P. (2004) Role of Phosphate and Carboxylate Ions in Maillard Browning. *J. Agric. Food Chem.*, **52**. https://doi.org/10.1021/jf030691t.

21. Chen, X. M. and Kitts, D. D. (2011) Identification and quantification of α-dicarbonyl compounds produced in different sugar-amino acid Maillard reaction model systems. *Food Research International*, **44**, 2775–2782. https://doi.org/10.1016/j.foodres.2011.06.002.

22. Dhungel, P., Bhattacherjee, A., Hrynets, Y. and Betti, M. (2020) The effect of amino acids on non-enzymatic browning of glucosamine: Generation of butterscotch aromatic and bioactive health compounds without detectable levels of neo-formed alkylimidazoles. *Food Chem.*,

308, 125612. https://doi.org/10.1016/j.foodchem.2019.125612.

23. Hrynets, Y., Ndagijimana, M. and Betti, M. (2015) Studies on the Formation of Maillard and Caramelization Products from Glucosamine Incubated at 37 °C. *J. Agric. Food Chem.*, **63**, 6249–6261. https://doi.org/10.1021/acs.jafc.5b02664.

24. Liu, P., Lu, X., Li, N., Zheng, Z. and Qiao, X. (2019) Characterization, variables, and antioxidant activity of the Maillard reaction in a fructose-histidine model system. *Molecules*, **24**. https://doi.org/10.3390/molecules24010056.

25. Zhang, X., Tao, N., Wang, X., Chen, F. and Wang, M. (2015) The colorants, antioxidants, and toxicants from nonenzymatic browning reactions and the impacts of dietary polyphenols on their thermal formation. *Food Funct.*, **6**. https://doi.org/10.1039/c4fo00996g.

26. Feng, T., Zhou, Y., Wang, X., Wang, X. and Xia, S. (2021) α-Dicarbonyl compounds related to antimicrobial and antioxidant activity of maillard reaction products derived from xylose, cysteine and corn peptide hydrolysate. *Food Biosci.*, **41**. https://doi.org/10.1016/j.fbio.2021.100951.

27. Zhao, L., Chen, J., Su, J., Li, L., Hu, S., Li, B., et al. (2013) In vitro antioxidant and anti-proliferative activities of 5-hydroxymethylfurfural. *J. Agric. Food Chem.*, **61**. https://doi.org/10.1021/jf403098y.

28. Tsai, P. J., Yu, T. Y., Chen, S. H., Liu, C. C. and Sun, Y. F. (2009) Interactive role of color and antioxidant capacity in caramels. *Food Research International*, **42**. https://doi.org/10.1016/j.foodres.2009.01.006.